Archival Report

Biological Psychiatry

Neuroprotective Peptide NAPVSIPQ Antagonizes Ethanol Inhibition of L1 Adhesion by Promoting the Dissociation of L1 and Ankyrin-G

Xiaowei Dou, Jerry Y. Lee, and Michael E. Charness

ABSTRACT

BACKGROUND: Ethanol causes developmental neurotoxicity partly by blocking adhesion mediated by the L1 neural cell adhesion molecule. This action of ethanol is antagonized by femtomolar concentrations of the neuropeptide NAPVSIPQ (NAP), an active fragment of the activity-dependent neuroprotective protein (ADNP). How femtomolar concentrations of NAP antagonize millimolar concentrations of ethanol is unknown. L1 sensitivity to ethanol requires L1 association with ankyrin-G; therefore, we asked whether NAP promotes the dissociation of ankyrin-G and L1.

METHODS: L1–ankyrin-G association was studied using immunoprecipitation, Western blotting, and immunofluorescence in NIH/3T3 cells transfected with wild-type and mutated human L1 genes. Phosphorylation of the ankyrin binding motif in the L1 cytoplasmic domain was studied after NAP treatment of intact cells, rat brain homogenates, and purified protein fragments.

RESULTS: Femtomolar concentrations of NAP stimulated the phosphorylation of tyrosine-1229 (L1-Y1229) at the ankyrin binding motif of the L1 cytoplasmic domain, leading to the dissociation of L1 from ankyrin-G and the spectrin-actin cytoskeleton. NAP increased the association of L1 and EphB2 and directly activated EphB2 phosphorylation of L1-Y1229. These actions of NAP were reproduced by P7A-NAP, a NAP variant that also blocks the teratogenic actions of ethanol, but not by I6A-NAP, which does not block ethanol teratogenesis as potently. Finally, knockdown of *EPHB2* prevented ethanol inhibition of L1 adhesion in NIH/3T3 cells.

CONCLUSIONS: NAP potently antagonizes ethanol inhibition of L1 adhesion by stimulating EphB2 phosphorylation of L1-Y1229. EphB2 plays a critical role in synaptic development; its potent activation by NAP suggests that ADNP may mediate synaptic development partly by activating EphB2.

Keywords: EphB2, Ethanol, L1, NAP, Phosphorylation, Y1229

https://doi.org/10.1016/j.biopsych.2019.08.020

Fetal alcohol spectrum disorders are highly prevalent causes of developmental disability (1,2). Brain lesions of fetal alcohol spectrum disorders resemble those of L1 syndrome, a disorder caused by mutations in the gene for the developmentally critical L1 neural cell adhesion molecule (3). This phenotypic similarity may be a consequence of the ability of ethanol to inhibit L1 adhesion at concentrations attained after just one drink (3). Ethanol interacts with an alcohol binding site in the extracellular domain of L1 (L1-ECD) at the interface between the Ig1 and Ig4 domains (4,5), a location essential for stabilizing a horseshoe conformation of L1 that favors L1 homophilic binding (6). The alcohol binding site discriminates the size and shape of diverse alcohols, and several alcohols antagonize ethanol inhibition of L1 adhesion (7). One such alcohol, 1-octanol, also interacts with the alcohol binding site (4) and prevents ethanol-induced growth retardation in mouse embryos at micromolar concentrations (8).

A second class of ethanol antagonists is exemplified by the peptides NAPVSIPQ (NAP) and SALLRSIPA (SAL). NAP and SAL are active fragments of the developmentally important activity-dependent neuroprotective protein (ADNP) and activity-dependent neurotrophic factor, respectively (9,10). Both NAP and SAL antagonize alcohol inhibition of L1 adhesion (11–13), and NAP protects against alcohol-induced growth retardation and delayed closure of the neural tube at femtomolar concentrations (12–14). ADNP and NAP may even protect against excessive alcohol consumption (15). Although NAP potently protects against a broad array of other central nervous system insults, NAP appears to block ethanol teratogenesis primarily by antagonizing ethanol inhibition of L1 adhesion, rather than through its broad neuroprotective actions (12). How femtomolar concentrations of NAP antagonize the actions of millimolar concentrations of ethanol is unknown. This stoichiometry strongly suggests that NAP acts through a catalytic mechanism, rather than by interacting directly with the alcohol binding site on the L1-ECD.

L1 sensitivity to ethanol requires the association of L1 with ankyrin-G and the spectrin-actin cytoskeleton (16,17). Linkage

of L1 to these cytoskeletal elements constrains the lateral mobility of L1 within the cell membrane (18), a change that is postulated to stabilize a conformation of the L1-ECD that favors the interaction of ethanol with the alcohol binding pocket (17). In contrast, dissociation of L1 from ankyrin-G and the spectrin-actin cytoskeleton increases the lateral mobility of L1, which may stabilize a conformation of the L1-ECD that excludes ethanol from the alcohol binding pocket. L1 association with ankyrin-G requires dephosphorylation of Y1229 within the L1 cytoplasmic domain (L1-CD) (19,20). Therefore, we asked whether NAP antagonizes ethanol inhibition of L1 adhesion by activating the phosphorylation of L1-Y1229, thereby promoting the dissociation of L1 and ankyrin. Here we show that NAP, but not octanol, potently induces the dissociation of L1 and ankyrin-G by activating EphB2, a kinase that phosphorylates L1-Y1229 (21,22). Moreover, knockdown of EphB2 abolishes NAP antagonism of ethanol inhibition of L1 adhesion.

METHODS AND MATERIALS

Reagents

The following antibodies were utilized: goat polyclonal antibody (pAb) against the L1-CD (SC-1508, RRID: AB_631086; Santa Cruz Biotechnology, Dallas, TX) (17,23,24), measuring total L1; monoclonal antibody (mAb) against the L1-ECD (SC-53386, UJ127, RRID: AB_628937; Santa Cruz Biotechnology) (25), measuring total L1; rabbit pAb against C-terminus of ankyrin-G (SC-28561, RRID: AB_633909; Santa Cruz Biotechnology) (17,26,27); mAb against L1 (5G3) (Maine Biotechnology Services, Portland, ME) (28); mAb against spectrin (SC-46696, RRID: AB_671135; Santa Cruz Biotechnology); goat pAb against actin (SC-1616, RRID: AB630836; Santa Cruz Biotechnology); mAb against EphB2 (SC-130752, RRID: AB_2099957; Santa Cruz Biotechnology); rabbit pAb against Src (SC-18, RRID: AB_631324; Santa Cruz Biotechnology); antibody mAb anti-phosphotyrosine (pY) (ab10321, RRID: AB_297058; Abcam, Cambridge, MA); horseradish peroxidase–conjugated secondary antibodies against mouse (115-035-062, RRID: AB_2338504; Jackson ImmunoResearch Laboratories, West Grove, PA), rabbit (711-035-152, RRID: AB_10015282; Jackson ImmunoResearch Laboratories), goat (705-035-003, RRID: AB_2340390; Jackson ImmunoResearch Laboratories); recombinant human EphB2 protein (PV3625) and kinase assay buffer (PV3189; Thermo Fisher Scientific, Waltham, MA); goat anti-mouse IgG conjugated with Alexa Fluor 546 (A-11003, RRID: AB_2534071; Thermo Fisher Scientific); goat anti-rabbit IgG conjugated with Alexa Fluor 488 (R37120, RRID: AB_2556548; Thermo Fisher Scientific); and mAb to β-tubulin (86298, RRID: AB_2715541; Cell Signaling Technology, Danvers, MA). NAP peptides were custom synthesized by New England Peptide Inc. (Gardner, MA); and CNEDGSFIGQYSGKKE (FIGQY) peptides were synthesized by GenScript USA Inc. (Piscataway, NJ).

Cell Culture

NIH/3T3 clonal cell line 2A2-L1$_s$ (ethanol-sensitive) stably expressing human L1 were employed to evaluate the effects of experimental manipulations on wild-type L1 (17), and NIH/3T3 cells transiently transfected with L1 mutations in the ankyrin binding region were used to study L1-ankyrin interactions, as described (20). Cells were cultured in Dulbecco's modified Eagle's medium plus 10% bovine serum (BS) at 37°C with 10% CO_2 atmosphere, as described (17).

Immunocytochemistry

NIH/3T3 cells were plated in 9-mm Petri dishes in Dulbecco's modified Eagle's medium supplemented with 10% BS and transiently transfected with wild-type L1 or L1-phenylalanine (Y1229F). After 48 hours of culture, cells were treated with 10^{-12} mol/L NAP for 1 hour and fixed in 4% paraformaldehyde for 30 minutes, blocked with phosphate-buffered saline (PBS) supplemented with 5% BS, and incubated overnight at 4°C with L1 mAb 5G3 (5) and rabbit pAb against ankyrin-G in PBS plus 5% BS. Cells were washed 3 times with PBS and incubated with goat anti-mouse IgG conjugated with Alexa Fluor 546 and goat anti-rabbit IgG conjugated with Alexa Fluor 488 in PBS with BS. Cells were washed again with PBS and fixed in paraformaldehyde. Images were captured using a Nikon Eclipse T*i* microscope (Nikon Instruments Inc., Melville, NY), and the colocalization efficiency of L1 and ankyrin-G were calculated using NIS-Elements Microscope Imaging Software (version 4.30; Nikon Instruments Inc.) (29).

Immunoprecipitation and Western Blot Analysis

Immunoprecipitation and Western blot analysis were carried out as described (17). NIH/3T3 cells were lysed in NP40 lysis buffer plus Halt Protease and Phosphatase Inhibitor Cocktail (1862495; Thermo Fisher Scientific). For L1 immunoprecipitation, whole cell lysates were incubated with mAb 5G3 (Maine Biotechnology Services) at 4°C for 2 to 4 hours, and protein A-agarose beads were added to precipitate the antigen-antibody complex. Images of protein bands were acquired on an Amersham Imager 600 (GE Healthcare Life Sciences, Pittsburgh, PA), and densitometry was quantified using ImageJ (National Institutes of Health, Bethesda, MD) (30,31). All data were normalized to values in 2A2-L1$_s$ cells or cells transfected with wild-type L1 (L1-WT) and plotted as mean ± SEM. The specificity of the L1 and ankyrin antibodies for immunoprecipitation and Western blotting is well established in the literature (17,23,32) and is further demonstrated in Supplemental Figures S1 and S2.

Small Interfering RNA Transfection of 2A2-L1$_s$ Cells

Cells were transfected with EphB2-siRNA (SC-39950; Santa Cruz Biotechnology), using Lipofectamine 2000 (Invitrogen, Carlsbad, CA) following the manufacturer's instructions (16). Scrambled small interfering RNA (siRNA) was used as a control, inactive siRNA (SC-37007; Santa Cruz Biotechnology). Forty-eight hours after transfection, cells were harvested for cell aggregation assays, Western blots, and coimmunoprecipitation analysis (16). Levels of protein expression in Western blots were normalized to values from untreated 2A2-L1$_s$ cells.

Preparation of Rat Brain Lysate

Rat brain lysates were prepared from whole brain homogenates of Sprague Dawley rat pups (Charles River Breeding, Worcester, MA) at postnatal day 10. Pups were euthanized in a

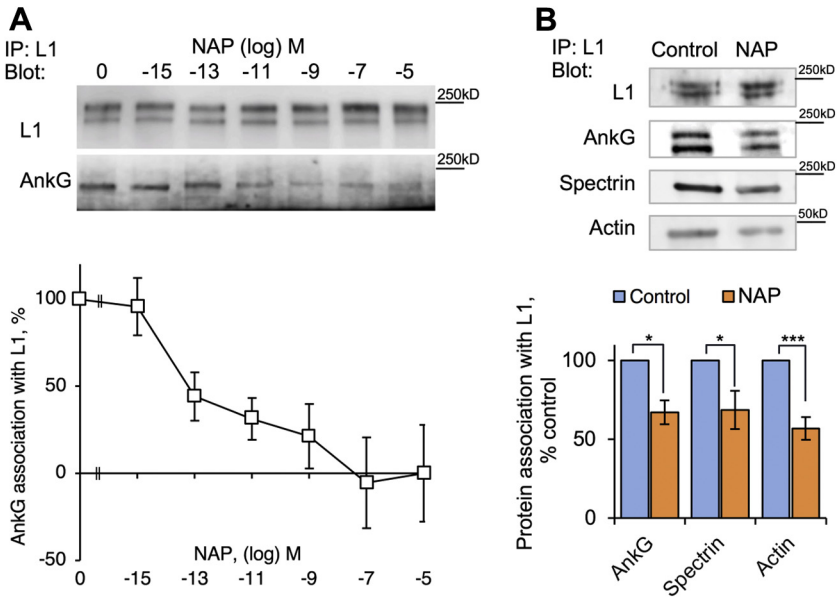

Figure 1. NAPVSIPQ (NAP) effect on the interaction of L1 with ankyrin-G (AnkG) and the spectrin-actin cytoskeleton. **(A)** L1 was immunoprecipitated (IP) using monoclonal antibody 5G3 from whole cell lysates of NIH/3T3 cells expressing human L1 (2A2-$L1_s$) that had been treated with NAP at various concentrations; coimmunoprecipitated proteins were separated and blotted with antibodies to L1 or AnkG. Ankyrin-G was detected as a band of approximately 190 kD, but occasionally, a second band was observed at approximately 150 kD, likely representing a splice variant (59). L1 was detected as a doublet at 210 kD and 190 kD. Protein band densities were normalized to values for total L1, and values were expressed as mean ± SEM percentage of control cells from 6 to 14 independent experiments ($F = 6.59$; $p < .0001$). **(B)** L1 was immunoprecipitated using monoclonal antibody 5G3 from whole cell lysates of 2A2-$L1_s$ cells treated with 10^{-9} mol/L (M) NAP, and coimmunoprecipitated proteins were separated and blotted with antibodies to L1, AnkG, spectrin, or actin. Protein band densities were normalized to values for total L1, and values were expressed as mean ± SEM percentage control cells from 5 to 13 independent experiments (AnkG: $^*t = 4.4$, $p = .01$; spectrin: $^*t = 2.6$; $p = .03$; actin: $^{***}t = 5.9$, $p = .0004$).

CO_2 chamber. The brain was removed, the cerebellum was dissected away, and the remaining tissue was frozen in liquid nitrogen. Thawed brain tissue was homogenized in NP40 lysis buffer plus protease and phosphatase inhibitors by repeated passage through a 20-gauge needle. After centrifugation, the supernatant was removed for coimmunoprecipitation experiments. The handling, care, and treatment of animals were performed in accordance with the guidelines of the Institutional Animal Care and Use Committee of VA Boston Healthcare System.

Cell Aggregation Assay

To perform cell aggregation assays, 2A2-$L1_s$ cells stably expressing human L1 or NIH/3T3 cells transiently transfected with L1 constructs were harvested, as described elsewhere (5,16). Cell aggregation assays were performed in the absence and presence of 100 mmol/L ethanol, a maximally effective concentration. Although the half maximal concentration for ethanol inhibition of L1 adhesion is ~5 mmol/L (3), we used high concentrations of ethanol to study the antagonist effects of NAP. Ethanol inhibition of L1 adhesion was normalized to values obtained in 2A2-$L1_s$ cells or the values obtained in cells transfected with L1-WT.

Phosphorylation of FIGQY Peptide

Phosphorylation of FIGQY-peptide by EphB2 kinase, whole cell lysate, or rat brain was performed on peptides conjugated to agarose beads according to the manufacturer's manual (26196, Pierce NHS-activated dry agarose beads; Thermo Fisher Scientific). Purified EphB2 (0.4 μg) protein or whole cell lysates (50 μg protein) were added to 2 μg of peptide-coated agarose beads in the absence or presence of NAP for the desired time in kinase buffer (PV3189; Thermo Fisher Scientific) supplemented with 2 mmol/L adenosine triphosphate at a final volume of 660 μL. The reaction was stopped by adding 1 mL PBS plus 2 mmol/L EDTA, and the particulate and supernatant fractions were separated by centrifugation at 3000 rev/min for 5 minutes at 4°C. The pellet was washed 3 times with 1 mL PBS, and incubated for 1 hour with anti-pY antibody ab10321 (Abcam) in 500 μL PBS plus 5% bovine serum albumin. After 3 washes, the pellet was denatured at 95°C in reducing sodium dodecyl sulfate sample buffer for Western blot analysis. Blotted membranes were incubated with horseradish peroxidase–conjugated secondary antibodies against mouse (115-035-062, RRID: AB_2338504), and the level of pY antibody retained on agarose beads was used as an index of tyrosine phosphorylation of FIGQY peptide.

Statistical Analysis

Data are expressed as mean ± SEM, except as noted. Statistical analysis was performed by using the analysis of variance and 2-tailed paired *t* tests using Prism 5 (GraphPad Software, San Diego, CA). Statistical significance was defined as $p < .05$. Levels of statistical significance were designated as follows: $^*p < .05$; $^{**}p < .01$; $^{***}p < .001$.

RESULTS

NAP Potently Reduces the Association of L1 With Ankyrin-G and the Spectrin-Actin Cytoskeleton

We evaluated the effects of NAP on L1 coupling to ankyrin-G using immunoprecipitation and Western blotting from NIH/3T3 cells transiently transfected with L1-WT. NAP caused a dose-dependent reduction in the association of WT-L1 with ankyrin-G (Figure 1A). Significant inhibition was observed at NAP concentrations of 100 fmol/L with maximal effects at 100 nmol/L. Treatment with 10^{-9} mol/L NAP also significantly decreased the association of L1 with spectrin and actin (Figure 1B).

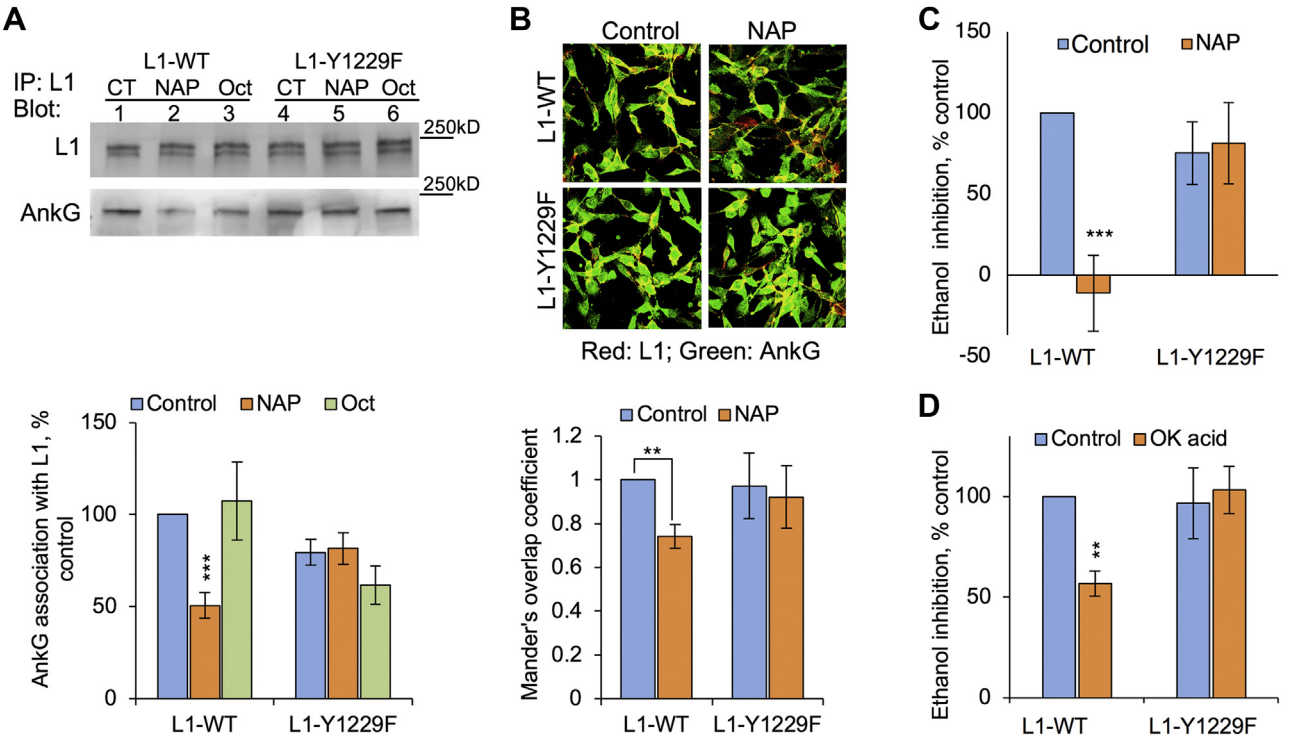

Figure 2. L1 association with ankyrin-G (AnkG) and ethanol inhibition of L1 adhesion in cells expressing wild-type L1 (L1-WT) or L1 in which Y1229 was mutated to phenylalanine (L1-Y1229F). **(A)** NIH/3T3 cells were transfected with L1-WT or L1-Y1229F in the absence (CT) and presence of 10^{-12} mol/L NAPVSIPQ (NAP) or 100 μmol/L octanol (Oct). L1 was immunoprecipitated (IP) from whole cell lysates using monoclonal antibody 5G3, and coimmunoprecipitated proteins were separated and blotted with antibodies to L1 and AnkG. Densities of AnkG bands were normalized to values for L1 in corresponding experiments and then expressed as a percentage of values in untreated cells expressing L1-WT. Shown are mean ± SEM percentage association of L1 and AnkG from 4 to 13 independent experiments ($F = 2.94$; $p < .05$); ***$t = 7.18$; $p < .001$. **(B)** Colocalization of L1 (red) and AnkG (green) immunostaining in L1-WT and L1-Y1229F–expressing cells treated for 1 hour in the absence and presence of 10^{-12} mol/L NAP. Mander's overlap coefficient indicated significant differences in the colocalization of L1 and AnkG under various experimental conditions ($F = 3.2$; $p < .05$); **$t = 5.26$; $p < .01$; $n = 14$ to 15. **(C, D)** The L1-Y1229F mutation abolished NAP (10^{-9} mol/L) and okadaic acid (OK) (100 μmol/L) antagonism of ethanol inhibition of L1 adhesion. NIH/3T3 cells were transiently transfected with L1-WT and L1-Y1229F. Cells were treated with 10^{-9} mol/L NAP or 100 μmol/L okadaic acid for 1 hour, and cells were harvested for cell aggregation assays performed in the absence and presence of 100 mmol/L ethanol. Ethanol inhibition of L1 adhesion in L1-Y1229F–expressing cells was expressed as a percentage of that obtained in L1-WT expressing cells (47.7 ± 4.4%). Shown are mean ± SEM relative levels of ethanol inhibition in **(C)** ($F = 16.77$; $p < .0001$); ***$t = 5.938$, $p = .0000$, $n = 12$ to 32; **(D)** ($F = 3.90$; $p < .05$); **$t = 6.93$; $p = 0.002$; $n = 5$. CT, control.

Interestingly, 100 μmol/L 1-octanol, a maximal antagonist concentration, had no significant effect on L1–ankyrin-G association (Figure 2A). These findings suggest that NAP and 1-octanol antagonize ethanol inhibition of L1 adhesion through different mechanisms.

L1-Y1229F Mutation Blocks the Actions of NAP on L1

Ankyrin-G binds to L1 at the consensus sequence FIGQY1229 in the L1-CD, and this binding requires dephosphorylation of L1-Y1229 (18,21). If NAP acts by inducing the dissociation of L1 and ankyrin-G, then stabilizing the association of L1 and ankyrin-G by preventing the phosphorylation of L1-Y1229 might eliminate NAP's antagonist activity. Mutation of Y1229 to Y1229F prevents phosphorylation at the 1229 site and stabilizes ankyrin-G association with L1 (17,20,33). We used this mutation to test whether NAP retains its antagonist properties when the residue at the 1229 position can no longer be phosphorylated. Immunoprecipitation studies showed that NAP had no effect on the association of ankyrin-G with L1-Y1229F, in contrast to its actions on L1-WT (Figure 2A). The effects of NAP on the colocalization of L1 and ankyrin-G were also visualized using immunofluorescence staining of L1 and ankyrin-G. As expected, NAP significantly reduced the colocalization of L1 and ankyrin-G in cells transfected with L1-WT but had no effect on their colocalization in cells transfected with L1-Y1229F (Figure 2B). Of note, both NAP and the phosphatase inhibitor okadaic acid blocked ethanol inhibition of L1 adhesion in cells transfected with L1-WT but not in cells transfected with L1-Y1229F (Figure 2C, D). These data imply that NAP promotes the dissociation of L1 and ankyrin-G and antagonizes ethanol inhibition of L1 adhesion by increasing the phosphorylation of L1-Y1229.

Lysates From NAP-Treated NIH/3T3 Cells or Rat Brain Increase Tyrosine Phosphorylation of FIGQY Peptide

We next sought evidence that NAP increases the phosphorylation of L1-Y1229. We were unable to raise an antibody that selectively recognizes phospho– or dephospho–L1-Y1229

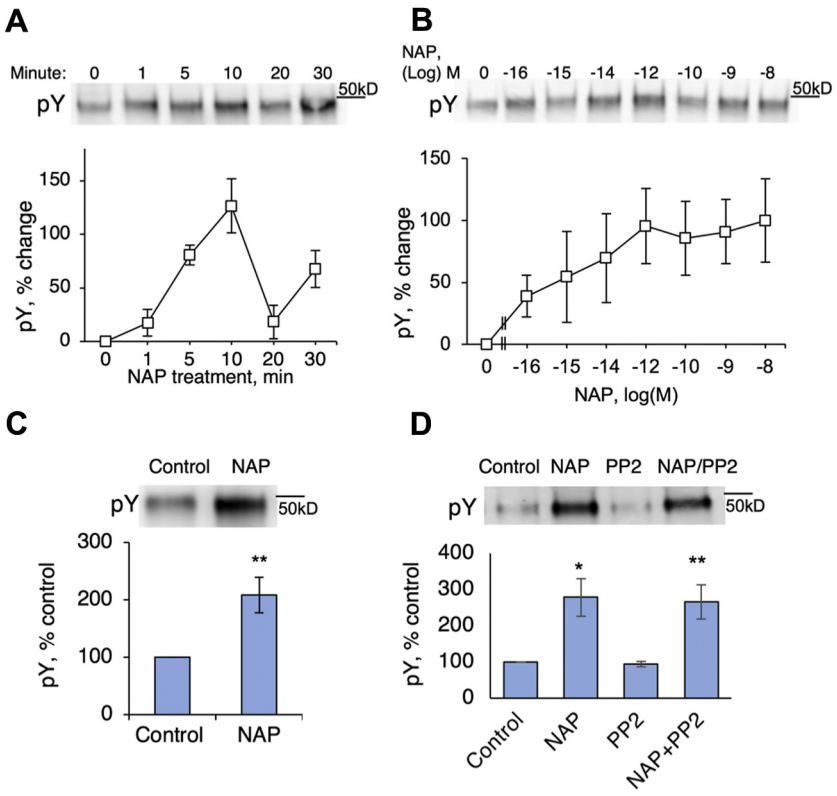

Figure 3. NAPVSIPQ (NAP) effect on tyrosine phosphorylation (pY) of the 16–amino acid CNEDGSFIGQYSGKKE (FIGQY) peptide fragment derived from the L1 cytoplasmic domain, containing a single tyrosine. **(A)** The 2A2-L1$_s$ cells were incubated in the absence and presence of 10^{-9} mol/L (M) NAP, and extracted cell lysates were incubated with FIGQY peptide conjugated to agarose beads at room temperature for the indicated time (see Methods and Materials). The pY of FIGQY peptide was measured using the mouse anti-pY monoclonal antibody PY20. The magnitude of pY in FIGQY peptide was quantified by densitometric analysis of anti-pY antibody-agarose bead bands separated by sodium dodecyl sulfate polyacrylamide gel electrophoresis. Densities of pY in the FIGQY peptide bands were normalized to values obtained at time 0. Shown are mean ± SEM percentage of pY of FIGQY peptide compared with values at time 0 from 5 independent experiments ($F = 9.84$; $p < .0001$). Peak phosphorylation occurred at 10 minutes following NAP treatment of intact cells. **(B)** Dose-response curve for NAP phosphorylation of FIGQY peptide by cell lysate from NAP-treated 2A2-L1$_s$ cells. Reactions were carried out for 10 minutes at room temperature in the presence of the indicated concentrations of NAP. The pY levels were normalized to values in cells that were not treated with NAP (lane 0). Shown is a representative gel from 12 experiments. Densitometry was obtained from 7 to 12 independent experiments ($F = 2.48$; $p < .05$). **(C)** Lysate of cerebral cortex from postnatal day 10 rat pups was incubated in the absence and presence of 10^{-12} M NAP for 10 minutes. NAP treatment of rat brain lysates significantly increased phosphorylation of FIGQY peptide (**$t = 2.888$; $p < .01$; $n = 7$). **(D)** The 2A2-L1$_s$ cells were incubated for 15 minutes at room temperature in the absence and presence of 10^{-9} M NAP and 20 μM PP2, and cell lysates were then incubated with FIGQY peptide to determine the effect of drug treatments on pY (*$t = 3.45$; $p = .010$; $n = 8$; and **$t = 3.55$; $p = .0085$; $n = 8$).

(21). Therefore, we used an anti-pY antibody to determine the phosphorylation state of a synthetic 16 amino acid peptide fragment of the L1-CD comprising a single tyrosine residue located within the FIGQY-ankyrin binding site (FIGQY peptide) (34). We used 2A2-L1$_s$, an ethanol-sensitive NIH/3T3 clonal cell line, because it stably expresses human L1 (16,17,35). We exposed 2A2-L1$_s$ cells to 10^{-9} mol/L NAP for various periods of time and then incubated whole cell lysates from NAP-treated 2A2-L1$_s$ cells with FIGQY peptide conjugated to agarose beads. Levels of phosphorylated FIGQY peptide were determined by Western blot analysis. NAP increased tyrosine phosphorylation of FIGQY peptide more than 2-fold, with peak effects occurring after 10 minutes of exposure (Figure 3A). A 10-minute NAP exposure caused a dose-dependent increase in FIGQY peptide phosphorylation, with significant effects observed at 10^{-16} mol/L and half maximal effects at approximately 3×10^{-15} mol/L (Figure 3B). NAP also caused a greater than 2-fold increase in FIGQY peptide phosphorylation in lysates from rat cerebral cortex (Figure 3C). These findings support the hypothesis that NAP acts by increasing the phosphorylation of L1-Y1229.

NAP Stimulates the Association of EphB2 and L1

The kinase EphB2 phosphorylates the FIGQY consensus sequence of L1 (21,22). We next asked whether NAP stimulates the association of EphB2 and L1 in NIH/3T3 cells transiently transfected with L1-WT. Treatment of these cells with 10^{-9} mol/L NAP significantly increased the association of L1 with EphB2, as determined by immunoprecipitation (Figure 4A). Hence, NAP treatment of intact cells brings EphB2 and L1 into proximity, thereby increasing the probability of EphB2 phosphorylation of L1-Y1229.

NAP and Its Active Homologues Stimulate EphB2 Phosphorylation of FIGQY Peptide

To determine whether NAP directly activates EphB2, we incubated purified EphB2 with FIGQY peptide in the absence and presence of various concentrations of NAP. NAP caused a dose-dependent increase in EphB2 phosphorylation of FIGQY peptide, with half maximal effects occurring between 10 and 100 fmol/L (Figure 4B). NAP did not increase phosphorylation of FIGQY peptide in the absence of EphB2.

Dai *et al.* (21) showed that EphB2 phosphorylation of L1-Y1229 in HEK293 cells is reduced by PP2, an Src family kinase inhibitor, suggesting that Src may be a downstream mediator of EphB2 phosphorylation of L1. In contrast, in our 2A2-L1$_s$ cells, 20 μmol/L PP2 had no effect on NAP stimulation of FIGQY peptide phosphorylation, both in whole cell lysates and with purified EphB2 (Figure 3D). Furthermore, NAP did not increase Src association with L1 in NIH/3T3 cells (69.8 ± 12.4% of control cells; $n = 6$; $p = .059$) (Supplemental Figure S3). These experiments suggest that in our model

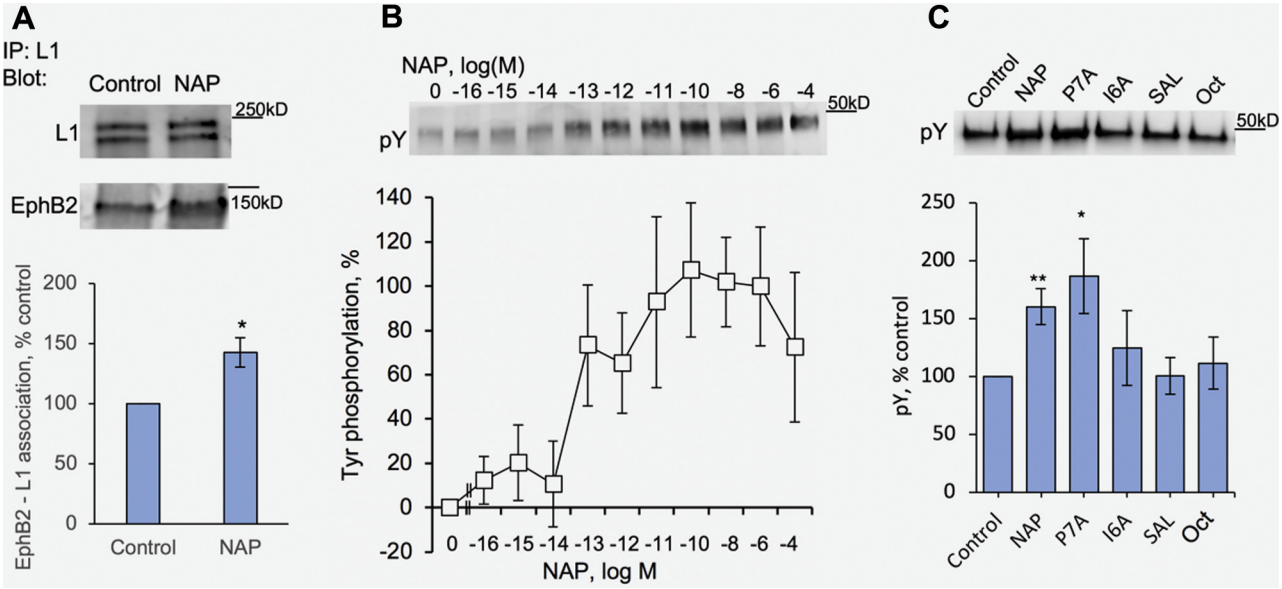

Figure 4. NAPVSIPQ (NAP) activation of EphB2 phosphorylation of L1. **(A)** Effect of NAP on association of L1 with EphB2. L1 was immunoprecipitated (IP) with monoclonal antibody 5G3 from 2A2-L1$_s$ cells in the absence and presence of 10^{-9} mol/L (M) NAP, and coimmunoprecipitated proteins were separated and blotted with antibodies to L1 and EphB2. Densities of EphB2 bands were normalized to those for L1, and values for NAP treatment were expressed as a percentage of control values. Shown is the mean ± SEM percentage increase in L1 association with EphB2 following NAP treatment derived from 8 to 9 independent experiments: $^*t = 3.17$; $p < .05$; $n = 8$. **(B)** Dose-dependent stimulation by NAP of tyrosine phosphorylation (pY) of CNEDGSFIGQYSGKKE peptide by recombinant EphB2 ($F = 2.45$; $p < .05$). The pY levels following NAP treatment were normalized to control values (0 NAP). Shown is the mean ± SEM percentage increase in pY levels following treatment with the indicated concentrations of NAP derived from 6 to 9 independent experiments. **(C)** Stimulation of EphB2 phosphorylation of L1 by 10^{-9} M NAP and P7A-NAP (P7A), but not by 10^{-9} M I6A-NAP (I6A), SALLRSIPA (SAL), or octanol (Oct). Shown is a representative gel and densitometric analysis from 7 independent experiments. The pY levels for each drug treatment were normalized to values obtained in the absence of drugs (Control) ($F = 2.84$; $p < .05$); $^*t = 3.01$; $p = .0235$; $^{**}t = 4.01$; $p = .0070$; $n = 7$.

system, NAP activates EphB2, and EphB2 directly phosphorylates L1.

A structure-activity analysis of NAP revealed that alanine replacement of proline (P7A-NAP) does not decrease NAP antagonism of ethanol inhibition of L1 adhesion or NAP inhibition of ethanol teratogenesis (12). In contrast, alanine replacement of isoleucine (I6A-NAP) greatly reduces both actions of NAP. Consistent with this structure-activity relationship, P7A-NAP was as effective as NAP in stimulating EphB2 phosphorylation of the FIGQY peptide, whereas I6A-NAP had no significant effect (Figure 4C). Neither SAL nor 1-octanol significantly activated EphB2 phosphorylation of FIGQY peptide.

Knockdown of EphB2 Blocks NAP Antagonism of Ethanol Inhibition of L1 Adhesion

If NAP antagonizes ethanol inhibition of L1 adhesion by stimulating EphB2 phosphorylation of L1-Y1229, then knockdown of EphB2 should reduce NAP antagonism. We transfected 2A2-L1$_s$ cells with an EphB2 siRNA, resulting in a 37 ± 9% reduction in EphB2 protein expression ($n = 9$; $p = .0047$) (Figure 5). This reduction in EphB2 expression abolished NAP stimulation of FIGQY peptide phosphorylation and eliminated NAP antagonism of ethanol inhibition of L1 adhesion. A scrambled siRNA had no effect on EphB2 expression or the actions of NAP.

DISCUSSION

These experiments identify a possible mechanism by which femtomolar concentrations of NAP antagonize the effects of millimolar concentrations of ethanol (Figure 6). NAP potently activates EphB2, leading to the association of EphB2 with L1 and the direct phosphorylation by EphB2 of Y1229 on the L1-CD. Phosphorylation of L1-Y1229 promotes the uncoupling of L1 from ankyrin-G and the spectrin-actin cytoskeleton. The resulting increase in lateral mobility of L1 in the cell membrane may then induce a conformational change in the L1-ECD that restricts access of ethanol to the alcohol binding pocket in the L1-ECD. In effect, an intracellular catalytic action of NAP produces an extracellular change that renders L1 insensitive to ethanol.

What is the evidence for this mechanism? Previous work demonstrated that L1 association with ankyrin-G was necessary for L1 sensitivity to ethanol (17). Phosphorylation of 4 separate residues on the L1-CD was required for ethanol inhibition of L1 adhesion (16,17). Each of these phosphorylation events led to an increase in L1 association with ankyrin-G and the spectrin-actin cytoskeleton. Dephosphorylation of each of these residues had no effect on L1 adhesion but reduced or abolished inhibition of L1 adhesion by ethanol, but not by methanol. The effects of dephosphorylation of these residues could be overcome by stabilizing the association of L1 and ankyrin-G through the mutation of L1-Y1229 to phenylalanine, a residue that cannot be phosphorylated. Furthermore, ethanol

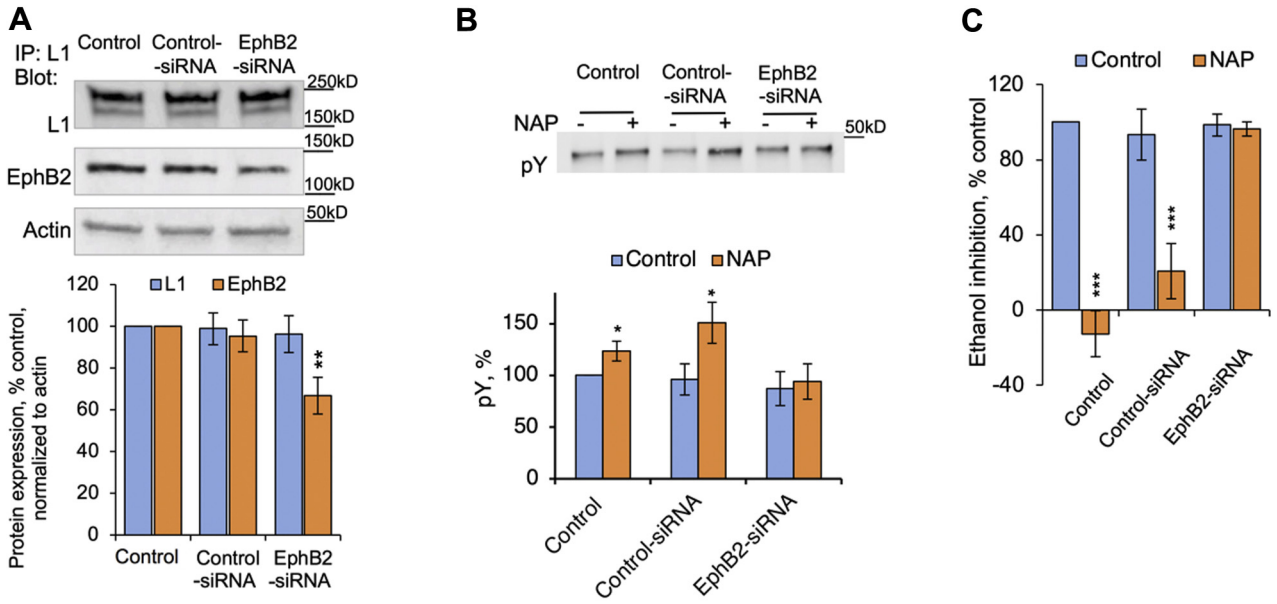

Figure 5. Effect of EphB2 knockdown on NAPVSIPQ (NAP) antagonism of ethanol inhibition of L1 adhesion. **(A)** The 2A2-L1$_s$ cells were treated with an EphB2 small interfering RNA (siRNA) or a scrambled siRNA. L1 and actin were used as loading control substances, and densities of protein bands were normalized to those obtained in untreated cells (Control). Shown is a representative gel and mean ± SEM percentage changes in EphB2 expression derived from 9 independent experiments ($F = 9.33$; $p < .001$); $^{**}t = 1.07$; $p < .0044$; $n = 10$. **(B)** EphB2 siRNA specifically reduced while scrambled siRNA had no effect on the phosphorylation of CNEDGSFIGQYSGKKE peptide from lysates of 2A2-L1$_s$ cells treated with 10^{-12} mol/L NAP. Values for tyrosine phosphorylation (pY) in NAP-treated siRNA-treated cells were normalized to values in control cells that were not treated with NAP ($F = 2.77$; $p < .05$); control: $^{*}t = 2.47$; $p = .04$; $n = 8$; control-siRNA: $^{*}t = 2.54$; $p = .039$; $n = 8$. **(C)** EphB2-siRNA specifically reduced while scrambled siRNA had no effect on NAP antagonism of ethanol inhibition of L1 adhesion. Values for ethanol inhibition of L1 adhesion in the presence of NAP were normalized to values obtained in the absence of NAP (38.6 ± 6.9%) ($F = 7.17$; $p < .0001$); control: $^{***}t = 9.30$; $p = .0000$; $n = 9$; control-siRNA: $^{***}t = 7.41$; $p = .0001$; $n = 9$. IP, immunoprecipitation.

inhibition of L1 adhesion could be abolished by knockdown of ankyrin-G. Collectively, these findings suggest that the dissociation of L1 from ankyrin-G leads to a small conformational change in the alcohol binding site in the L1-ECD that excludes ethanol (17).

Ankyrin-G binds to L1 at the highly conserved consensus sequence FIGQY1229 only when Y1229 is dephosphorylated (18,36). Because ankyrin binding to L1 is necessary for ethanol inhibition of L1 adhesion, drugs that stimulate the phosphorylation or inhibit the dephosphorylation of Y1229 will antagonize ethanol inhibition of L1 adhesion. We found that okadaic acid, a phosphatase inhibitor, blocked ethanol inhibition of L1-WT adhesion but had no effect on ethanol inhibition of L1-Y1229F adhesion. These findings imply that okadaic acid antagonizes ethanol inhibition of L1 adhesion by inhibiting dephosphorylation of L1-Y1229. Our data do not indicate whether NAP also acts as a phosphatase inhibitor; however, we found strong evidence that NAP antagonizes ethanol inhibition of L1 adhesion by stimulating the phosphorylation of Y1229.

NAP stimulated the dissociation of L1 and ankyrin-G at femtomolar concentrations. The potency of NAP for inducing the dissociation of ankyrin-G and L1 was comparable to that observed for NAP antagonism of ethanol inhibition of L1 adhesion (11–13), consistent with a common mechanism of action. Like okadaic acid, NAP did not reduce ethanol inhibition of L1-Y1229F adhesion or promote the dissociation of L1-Y1229F and ankyrin-G. These findings support the hypothesis that NAP antagonizes ethanol inhibition of L1 adhesion by increasing the phosphorylation of L1-Y1229 and promoting the dissociation of L1 and ankyrin.

We were not able to raise antibodies that would have allowed us to measure phosphorylation of Y1229 as part of the full L1 molecule within intact cells. Rather, our assay depended on the detection of tyrosine phosphorylation of a peptide fragment of L1 that contained Y1229 as the sole tyrosine, an approach that has proven effective in other proteins (34). Past work showing phosphorylation of L1 by EphB2 in intact cells increases the likelihood that our in vitro phosphorylation assay reflects in vivo events. Our data identify EphB2 as a kinase that NAP activates to phosphorylate Y1229. The ability to block the antagonist action of NAP by partial knockdown of EphB2 in intact cells further implies that NAP activation of EphB2 and EphB2 phosphorylation of L1-Y1229 constitute the primary mechanism responsible for NAP antagonism of ethanol inhibition of L1 adhesion.

NAP treatment of mouse embryos prevents ethanol-induced fetal demise, growth retardation, premature closure of the neural tube, and cognitive deficits in adult mice (12,14,37,38). NAP may decrease ethanol embryotoxicity through diverse mechanisms, including reducing ethanol-induced increases in proinflammatory cytokines (37,39), decreases in vasoactive intestinal peptide (40) and brain-derived neurotrophic factor (41), neuroprotection (42), and antagonism of ethanol inhibition of L1 adhesion (12). Systematic replacement of individual amino acids of NAP with alanine produced a series of NAP homologues that

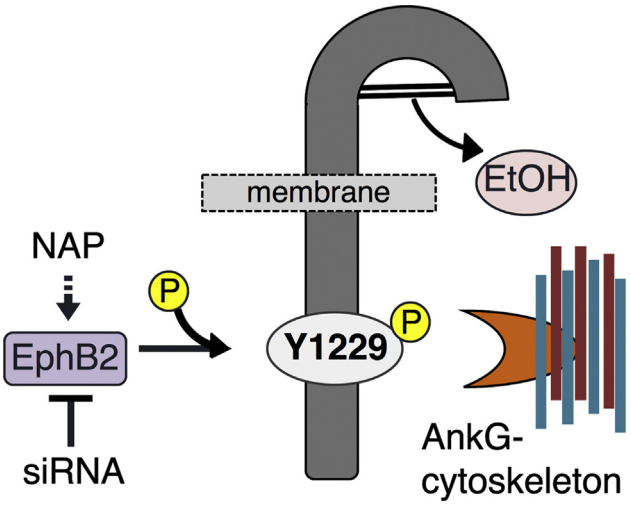

Figure 6. NAPVSIPQ (NAP) antagonizes ethanol inhibition of L1 adhesion by activating EphB2 phosphorylation (P) of L1-Y1229, leading to the dissociation of L1 from ankyrin-G (AnkG) and the spectrin-actin cytoskeleton. L1 is sensitive to ethanol (EtOH) only when it is associated with ankyrin-G. siRNA, small interfering RNA.

differed markedly in their antagonism of ethanol inhibition of L1 adhesion and their inhibition of tetrodotoxin neurotoxicity (neuroprotection) (12). P7A-NAP abolished NAP neuroprotection but did not reduce antagonism of either ethanol inhibition of L1 adhesion or embryotoxicity. In contrast, I6A-NAP preserved neuroprotection but greatly reduced antagonism of both ethanol inhibition of L1 adhesion and embryotoxicity. These findings suggested that NAP antagonism of ethanol inhibition of L1 adhesion was more important than neuroprotection in preventing ethanol embryotoxicity in mice (12). Our current experiments demonstrate that P7A-NAP is also more effective than I6A-NAP in stimulating the phosphorylation of L1-Y1229. These findings suggest that NAP stimulation of L1-Y1229 phosphorylation plays a pivotal role in preventing ethanol embryotoxicity in mice. In contrast, the neuroprotective peptide SAL did not activate L1-Y1229 phosphorylation and may therefore prevent ethanol embryotoxicity (43) through a different mechanism.

NAP directly stimulated the activation of EphB2, leading to phosphorylation of L1-Y1229. In our experiments, EphB2 appeared to phosphorylate L1-Y1229 directly. In contrast, EphB2 phosphorylation of L1-Y1229 in HEK293 cells requires activation of Src (21). We could not block EphB2 activation of L1-Y1229 phosphorylation with the Src family kinase inhibitor PP2, and we did not find that NAP promoted the association of Src with L1 in NIH/3T3 cells. Therefore, this activation does not appear to be necessary for NAP activation of EphB2 or EphB2 phosphorylation of L1-Y1229, at least in our model system.

Octanol also antagonizes ethanol inhibition of L1 adhesion (7); however, it appears to do so by a different mechanism than NAP. NAP stimulated the dissociation of L1 and ankyrin-G and stimulated EphB2 phosphorylation of FIGQY peptide, whereas 1-octanol showed neither of those effects. Previous work demonstrated that 1-octanol interacts directly with the alcohol binding pocket in the L1-ECD (4). The effective concentrations of 1-octanol and ethanol are more similar than those for NAP and ethanol, and based on differences in membrane-buffer partition coefficient, the membrane concentration of 10 μmol/L 1-octanol and 100 mmol/L ethanol are likely very similar (7). Hence, 1-octanol may act as a competitive antagonist, whereas NAP may act noncompetitively through a catalytic mechanism.

The Eph family of signaling molecules are receptor tyrosine kinases that interact with ephrins on adjacent cellular processes to promote bidirectional signaling (44,45). EphB2 and its ephrin ligands guide pathfinding of neuronal growth cones (45,46), and EphB2 plays a critical role in synapse formation and synaptic stabilization (45). The kinetics of EphB2 activation in cortical dendritic filopodia mediates the sampling and selection of axonal processes for synapse formation (47).

The interaction of EphB2 and L1 contributes to forward signaling in hippocampal development (46) and in retinocollicular synaptic mapping (21). Disruption of the EphB2 signaling pathway leads to aberrant retinocollicular mapping. Furthermore, deletions of the genes for the EphB2, EphB3, and L1 lead to defective pathfinding of commissural axons, resulting in agenesis of the anterior commissure or the corpus callosum (48–50). Dysgenesis of the corpus callosum also occurs in fetal alcohol spectrum disorders (51), perhaps reflecting the linkage between ethanol inhibition of L1 adhesion and ethanol embryotoxicity (3).

NAP is an active motif of ADNP, a molecule that is critical for normal development (52,53). *ADNP* gene mutations are among the most common genetic abnormalities in autism spectrum disorder (54), which arises in part due to abnormal synaptic formation. ADNP regulates the activity of numerous genes by chromatin remodeling (55). Among its many actions, NAP is believed to strengthen synaptic connections by binding to microtubule end-binding proteins and promoting axonal transport (9). The potent activation of EphB2 by NAP suggests that ADNP may mediate normal synaptic development in part by stimulating EphB2 activity. EphB1 is a microtubule-associated protein (56), and it is conceivable that the cognate Eph ligands interact with ephrins on a microtubule scaffold. Indeed, there is evidence that EphB2 may help shape dendritic morphogenesis through its interaction with GRIP1 and kinesin-1, a microtubule motor protein (57). Hence, NAP might activate EphB2 through its interaction with microtubules or other microtubule-associated proteins (58). Further work is necessary to support this hypothesis.

ACKNOWLEDGMENTS AND DISCLOSURES

This work was supported by National Institute on Alcohol Abuse and Alcoholism (NIAAA) Grant No. R01AA012974 (to MEC), NIAAA Grant No. U24AA014811 as a component of the Collaborative Initiative on Fetal Alcohol Spectrum Disorders (CIFASD) (to MEC); The Medical Research Service and Veterans Affairs Merit Review Grant No. 5I01BX002374 (to MEC); Department of Defense Grant No. W81XWH-12-2-0048 Subaward No. 8742sc (to MEC). Part of this work was done in conjunction with the CIFASD, which is funded by grants from the National Institute on Alcohol Abuse and Alcoholism. Additional information about CIFASD can be found at www.cifasd.org.

The authors report no biomedical financial interests or potential conflicts of interest.

ARTICLE INFORMATION

From the Department of Neurology, Veterans Affairs Boston Healthcare System (XD, JYL, MEC), West Roxbury; Department of Neurology (XD, JYL, MEC), Harvard Medical School, Boston; and Department of Neurology (MEC), Boston University School of Medicine, Boston, Massachusetts.

Address correspondence to Michael E. Charness, M.D., 1400 VFW Parkway, West Roxbury, MA 02132; E-mail: mcharness@hms.harvard.edu.

Received Jun 10, 2019; revised and accepted Aug 21, 2019.

Supplementary material cited in this article is available online at https://doi.org/10.1016/j.biopsych.2019.08.020.

REFERENCES

1. May PA, Chambers CD, Kalberg WO, Zellner J, Feldman H, Buckley D, *et al.* (2018): Prevalence of fetal alcohol spectrum disorders in 4 US communities. JAMA 319:474–482.
2. Wozniak JR, Riley EP, Charness ME (2019): Clinical presentation, diagnosis, and management of fetal alcohol spectrum disorder. Lancet Neurol 18:760–770.
3. Ramanathan R, Wilkemeyer MF, Mittal B, Perides G, Charness ME (1996): Ethanol inhibits cell-cell adhesion mediated by human L1. J Cell Biol 133:381–390.
4. Arevalo E, Shanmugasundararaj S, Wilkemeyer MF, Dou X, Chen S, Charness ME, *et al.* (2008): An alcohol binding site on the neural cell adhesion molecule L1. Proc Natl Acad Sci U S A 105:371–375.
5. Dou X, Menkari CE, Shanmugasundararaj S, Miller KW, Charness ME (2011): Two alcohol binding residues interact across a domain interface of the L1 neural cell adhesion molecule and regulate cell adhesion. J Biol Chem 286:16131–16139.
6. Haspel J, Grumet M (2003): The L1CAM extracellular region: A multi-domain protein with modular and cooperative binding modes. Front Biosci 8:1210–1225.
7. Wilkemeyer MF, Sebastian AB, Smith SA, Charness ME (2000): Antagonists of alcohol inhibition of cell adhesion. Proc Natl Acad Sci U S A 97:3690–3695.
8. Chen S-Y, Wilkemeyer MF, Sulik KK, Charness ME (2001): Octanol antagonism of ethanol teratogenesis. FASEB J 15:1649–1651.
9. Oz S, Kapitansky O, Ivashco-Pachima Y, Malishkevich A, Giladi E, Skalka N, *et al.* (2014): The NAP motif of activity-dependent neuroprotective protein (ADNP) regulates dendritic spines through microtubule end binding proteins. Mol Psychiatry 19:1115–1124.
10. Gozes I, Brenneman DE (1996): Activity-dependent neurotrophic factor (ADNF): An extracellular neuroprotective chaperonin? J Mol Neurosci 7:235–244.
11. Wilkemeyer MF, Chen SY, Menkari C, Sulik KK, Charness ME (2004): Ethanol antagonist peptides: Structural specificity without stereospecificity. J Pharmacol Exp Ther 309:1183–1189.
12. Wilkemeyer MF, Chen SY, Menkari C, Brenneman D, Sulik KK, Charness ME (2003): Differential effects of ethanol antagonism and neuroprotection in peptide fragment NAPVSIPQ prevention of ethanol-induced developmental toxicity. Proc Natl Acad Sci U S A 100:8543–8548.
13. Wilkemeyer MF, Menkari C, Spong CY, Charness ME (2002): Peptide antagonists of ethanol inhibition of L1-mediated cell-cell adhesion. J Pharmacol Exp Ther 303:110–116.
14. Spong CY, Abebe DT, Gozes I, Brenneman DE, Hill JM (2001): Prevention of fetal demise and growth restriction in a mouse model of fetal alcohol syndrome. J Pharmacol Exp Ther 297:774–779.
15. Ziv Y, Rahamim N, Lezmy N, Even-Chen O, Shaham O, Malishkevich A, *et al.* (2019): Activity-dependent neuroprotective protein (ADNP) is an alcohol-responsive gene and negative regulator of alcohol consumption in female mice. Neuropsychopharmacology 44:415–424.
16. Dou X, Wilkemeyer MF, Menkari CE, Parnell SE, Sulik KK, Charness ME (2013): Mitogen-activated protein kinase modulates ethanol inhibition of cell adhesion mediated by the L1 neural cell adhesion molecule. Proc Natl Acad Sci U S A 110:5683–5688.
17. Dou X, Menkari C, Mitsuyama R, Foroud T, Wetherill L, Hammond P, *et al.* (2018): L1 coupling to ankyrin and the spectrin-actin cytoskeleton modulates ethanol inhibition of L1 adhesion and ethanol teratogenesis. FASEB J 32:1364–1374.
18. Garver TD, Ren Q, Tuvia S, Bennett V (1997): Tyrosine phosphorylation at a site highly conserved in the L1 family of cell adhesion molecules abolishes ankyrin binding and increases lateral mobility of neurofascin. J Cell Biol 137:703–714.
19. Buhusi M, Schlatter MC, Demyanenko GP, Thresher R, Maness PF (2008): L1 interaction with ankyrin regulates mediolateral topography in the retinocollicular projection. J Neurosci 28:177–188.
20. Needham LK, Thelen K, Maness PF (2001): Cytoplasmic domain mutations of the L1 cell adhesion molecule reduce L1-ankyrin interactions. J Neurosci 21:1490–1500.
21. Dai J, Dalal JS, Thakar S, Henkemeyer M, Lemmon VP, Harunaga JS, *et al.* (2012): EphB regulates L1 phosphorylation during retinocollicular mapping. Mol Cell Neurosci 50:201–210.
22. Zisch AH, Stallcup WB, Chong LD, Dahlinhuppe K, Voshol J, Schachner M, *et al.* (1997): Tyrosine phosphorylation of L1 family adhesion molecules: Implication of the Eph Kinase Cek5. J Neurosci Res 47:655–665.
23. Tagliavacca L, Colombo F, Racchetti G, Meldolesi J (2013): L1CAM and its cell-surface mutants: New mechanisms and effects relevant to the physiology and pathology of neural cells. J Neurochem 124:397–409.
24. Li Y, Galileo DS (2010): Soluble L1CAM promotes breast cancer cell adhesion and migration in vitro, but not invasion. Cancer Cell Int 10:34.
25. Chen MM, Lee CY, Leland HA, Lin GY, Montgomery AM, Silletti S (2010): Inside-out regulation of L1 conformation, integrin binding, proteolysis, and concomitant cell migration. Mol Biol Cell 21:1671–1685.
26. Silva E, Soares-da-Silva P (2009): Protein cytoskeleton and overexpression of Na+,K+-ATPase in opossum kidney cells. J Cell Physiol 221:318–324.
27. Zhu S, Cordner ZA, Xiong J, Chiu C-T, Artola A, Zuo Y, *et al.* (2017): Genetic disruption of ankyrin-G in adult mouse forebrain causes cortical synapse alteration and behavior reminiscent of bipolar disorder. Proc Natl Acad Sci U S A 114:10479–10484.
28. Mujoo K, Spiro RC, Reisfeld RA (1986): Characterization of a unique glycoprotein antigen expressed on the surface of human neuroblastoma cells. J Biol Chem 261:10299–10305.
29. Dunn KW, Kamocka MM, McDonald JH (2011): A practical guide to evaluating colocalization in biological microscopy. Am J Physiol Cell Physiol 300:C723–C742.
30. Schindelin J, Rueden CT, Hiner MC, Eliceiri KW (2015): The ImageJ ecosystem: An open platform for biomedical image analysis. Mol Reprod Dev 82:518–529.
31. Schneider CA, Rasband WS, Eliceiri KW (2012): NIH Image to ImageJ: 25 years of image analysis. Nat Methods 9:671–675.
32. Leussis MP, Berry-Scott EM, Saito M, Jhuang H, de Haan G, Alkan O, *et al.* (2013): The ANK3 bipolar disorder gene regulates psychiatric-related behaviors that are modulated by lithium and stress. Biol Psychiatry 73:683–690.
33. Zhang X, Davis JQ, Carpenter S, Bennett V (1998): Structural requirements for association of neurofascin with ankyrin. J Biol Chem 273:30785–30794.
34. Lind J, Backert S, Hoffmann R, Eichler J, Yamaoka Y, Perez-Perez GI, *et al.* (2016): Systematic analysis of phosphotyrosine antibodies recognizing single phosphorylated EPIYA-motifs in CagA of East Asian-type Helicobacter pylori strains. BMC Microbiol 16:201.
35. Wilkemeyer MF, Charness ME (1998): Characterization of alcohol-sensitive and insensitive fibroblast cell lines expressing human L1. J Neurochem 71:2382–2391.
36. Tuvia S, Garver TD, Bennett V (1997): The phosphorylation state of the FIGQY tyrosine of neurofascin determines ankyrin-binding activity and patterns of cell segregation. Proc Natl Acad Sci U S A 94:12957–12962.
37. Vink J, Auth J, Abebe DT, Brenneman DE, Spong CY (2005): Novel peptides prevent alcohol-induced spatial learning deficits and proinflammatory cytokine release in a mouse model of fetal alcohol syndrome. Am J Obstet Gynecol 193:825–829.
38. Chen SY, Charness ME, Wilkemeyer MF, Sulik KK (2005): Peptide-mediated protection from ethanol-induced neural tube defects. Dev Neurosci 27:13–19.
39. Roberson R, Kuddo T, Benassou I, Abebe D, Spong CY (2012): Neuroprotective peptides influence cytokine and chemokine alterations in a model of fetal alcohol syndrome. Am J Obstet Gynecol 207:499.e491-495.

40. Spong CY, Auth J, Vink J, Goodwin K, Abebe DT, Hill JM, *et al.* (2002): Vasoactive intestinal peptide mRNA and immunoreactivity are decreased in fetal alcohol syndrome model. Regul Pept 108:143–147.
41. Incerti M, Vink J, Roberson R, Benassou I, Abebe D, Spong CY (2010): Prevention of the alcohol-induced changes in brain-derived neurotrophic factor expression using neuroprotective peptides in a model of fetal alcohol syndrome. Am J Obstet Gynecol 202:457.e451-454.
42. Gozes I, Brenneman DE (2000): A new concept in the pharmacology of neuroprotection. J Mol Neurosci 14:61–68.
43. Zhou FC, Sari Y, Powrozek TA, Spong CY (2004): A neuroprotective peptide antagonizes fetal alcohol exposure-compromised brain growth. J Mol Neurosci 24:189–199.
44. Kullander K, Klein R (2002): Mechanisms and functions of Eph and ephrin signalling. Nat Rev Mol Cell Biol 3:475–486.
45. Henderson NT, Dalva MB (2018): EphBs and ephrin-Bs: Trans-synaptic organizers of synapse development and function. Mol Cell Neurosci 91:108–121.
46. Robichaux MA, Chenaux G, Ho HY, Soskis MJ, Dravis C, Kwan KY, *et al.* (2014): EphB receptor forward signaling regulates area-specific reciprocal thalamic and cortical axon pathfinding. Proc Natl Acad Sci U S A 111:2188–2193.
47. Mao YT, Zhu JX, Hanamura K, Iurilli G, Datta SR, Dalva MB (2018): Filopodia conduct target selection in cortical neurons using differences in signal kinetics of a single kinase. Neuron 98:767–782 e768.
48. Orioli D, Henkemeyer M, Lemke G, Klein R, Pawson T (1996): Sek4 and Nuk receptors cooperate in guidance of commissural axons and in palate formation. EMBO J 15:6035–6049.
49. Henkemeyer M, Orioli D, Henderson JT, Saxton TM, Roder J, Pawson T, *et al.* (1996): Nuk controls pathfinding of commissural axons in the mammalian central nervous system. Cell 86:35–46.
50. Fransen E, Lemmon V, Vancamp G, Vits L, Coucke P, Willems PJ (1995): CRASH syndrome: Clinical spectrum of corpus callosum hypoplasia, retardation, adducted thumbs, spastic paraparesis and hydrocephalus due to mutations in one single gene, L1. Eur J Hum Genet 3:273–284.
51. Riley EP, Mattson SN, Sowell ER, Jernigan TL, Sobel DF, Jones KL (1995): Abnormalities of the corpus callosum in children prenatally exposed to alcohol. Alcohol Clin Exp Res 19:1198–1202.
52. Zemlyak I, Furman S, Brenneman DE, Gozes I (2000): A novel peptide prevents death in enriched neuronal cultures. Regul Pept 96:39–43.
53. Gozes I (2007): Activity-dependent neuroprotective protein: From gene to drug candidate. Pharmacol Ther 114:146–154.
54. Arnett AB, Rhoads CL, Hoekzema K, Turner TN, Gerdts J, Wallace AS, *et al.* (2018): The autism spectrum phenotype in ADNP syndrome. Autism Res 11:1300–1310.
55. Mandel S, Gozes I (2007): Activity-dependent neuroprotective protein constitutes a novel element in the SWI/SNF chromatin remodeling complex. J Biol Chem 282:34448–34456.
56. Colbert PL, Vermeer DW, Wieking BG, Lee JH, Vermeer PD (2015): EphrinB1: Novel microtubule associated protein whose expression affects taxane sensitivity. Oncotarget 6:953–968.
57. Hoogenraad CC, Milstein AD, Ethell IM, Henkemeyer M, Sheng M (2005): GRIP1 controls dendrite morphogenesis by regulating EphB receptor trafficking. Nat Neurosci 8:906–915.
58. Ivashko-Pachima Y, Sayas CL, Malishkevich A, Gozes I (2017): ADNP/NAP dramatically increase microtubule end-binding protein–Tau interaction: A novel avenue for protection against tauopathy. Mol Psychiatry 22:1335.
59. Nelson AD, Jenkins PM (2016): The splice is right: ANK3 and the control of cortical circuits. Biol Psychiatry 80:263–265.